Bull. Chem. Soc. Ethiop. **2016**, 30(2), 231-239.
Printed in Ethiopia
DOI: http://dx.doi.org/10.4314/bcse.v30i2.7
ISSN 1011-3924
© 2016 Chemical Society of Ethiopia

STRUCTURAL AND SPECTROSCOPIC STUDIES OF 2,9-DIMETHYL-1,10-PHENANTHROLINIUM CATION (DPH) WITH CHLORIDE, TRIFLATE AND GOLD DICYANIDE ANIONS. THE ROLE OF H-BONDING IN MOLECULAR RECOGNITION AND ENHANCEMENT OF π-π STACKING

Zerihun Assefa* and Shaka B. Gore

Chemistry Department, North Carolina A&T State University Greensboro, NC 27411, USA

(Received June 19, 2015; revised February 29, 2016)

ABSTRACT. The crystal structures of the pronated ligand, 2,9-dimethyl-1,10-phenanthrolinium (DPH) cation with selected counter anions (chloride (**1**), triflate (**2**), and gold dicyanide (**3**)) are reported. The role of a hydrogen bond interaction in influencing the solid state π-π stacking found in all three compounds has been investigated. In the chloride, and triflate adducts **1** and **2**, respectively, the solid state morphology was stabilized by additional H-bonding interaction. In particular, compound **1** displays extensive network of H-bonding interaction where π–π stacked layers are interlinked through the H-bonding network. In compound **2**, the H-bonding interaction is less pronounced and involves mainly the non-coordinating triflate anion and the protonated N atom of the cation connecting neighboring intra-layer molecules. In **3** a weaker interaction exists between the N atom of the $Au(CN)_2^-$ anion and the protonated N of the ligand, but the system lacks extensive intra- or inter-layer H-bonding interaction that connects the neighboring molecules.

KEY WORDS: Phenanthroline, H-bonding, X-ray structure, π- π stacking

INTRODUCTION

Phenanthroline (phen) and its derivatives comprise an important class of chelating ligands and are popular Lewis bases because of their N-donor ability [1-3]. Phen is a rigid, conjugated, tricyclic molecule, planar, hydrophobic, and electron-poor heteroaromatic system which has two pyridine rings connected to a central benzene ring making charge interjection and transporting easier [4-6]. Being a convenient Lewis base [7-8] it is able to form octahedral complexes such as $[M(phen)(H_2O)_4]^{2+}$, $[M(phen)_2(H_2O)_2]^{2+}$ and $[M(phen)_3]^{2+}$ with first row transition metal cations. Compared to the parent 2,2-bipyridine (bpy), or 2,2,6,6-terpyridine (tpy) systems, the phen derivative 2,9-dimethyl-1,10-phenanthroline (DPH) is characterized by two inward-pointing nitrogen donor atoms, pre-organized for strong and entropically favored metal binding. A similar disposition of the nitrogen donors in bpy and tpy can be disrupted by the free rotation about the bond(s) linking the heteroaromatic six-membered rings.

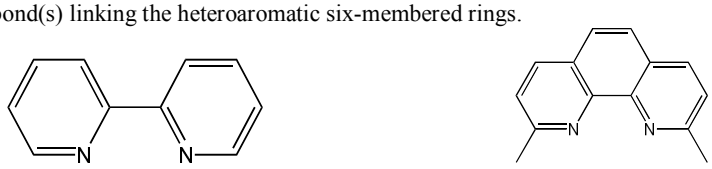

bpy DPH

Scheme 1. Structural comparison of bipyridine (bpy) and phen based ligand DPH.

Electronically the chelating bpy and DPH are in particular unique in their electron deficiency [9, 10] and hence, are excellent π–acceptors capable of stabilizing metal ions in lower oxidation states. Due to the presence of low-energy π* orbitals of the ligand, metal

*Corresponding author. E-mail: zassefa@ncat.edu

complexes can be characterized by strong metal-to-ligand charge-transfer (MLCT) absorption bands in the visible spectrum and hence a red-shifted fluorescent emission should be expected [11, 12]. Many of the extraordinary molecular architectures such as catenanes, rotaxane and knots owe their appearance in the literature due to the coordinating properties of phen [13-16].

In this study the structural features of the protonated DPH system with the chloride, triflate, and gold dicyanide anions is described along with their spectroscopic properties.

EXPERIMENTAL

*Synthesis of [(DPH)Cl]•3H_2O (**1**)*

Crystals of this compound were obtained as a byproduct of a synthetic attempt to coordinate lanthanide chloride to the DPH ligand. A 0.13 mmol of $TbCl_3$•6H_2O, and 0.13 mmol of DPH were dissolved separately, in 10 mL of MeOH in round bottom flask and in 4 mL of MeOH, respectively. The DPH ligand was added drop wise to the lanthanide solution. The reaction mixture was stirred for several hours and filtered through celite and evaporated under vacuum. The solid white product collected was recrystallized from MeOH and placed in a fume hood for slow evaporation. Clear X-ray quality crystals of the unexpected compound **1** were obtained after several days.

Similarly, compound **2** was also obtained unintentionally when the triflate salt of the lanthaide ($Eu(CF_3O_3S)_3$) was used in a similar synthetic scheme as described above for compound **1**.

*Synthesis of [(DPH)Au(CN)$_2$)]•H_2O (**3**)*

In a 20 mL beaker a 0.08 mmol of $KAu(CN)_2$ was dissolved in 3 mL of distilled H_2O. In another 20 mL beaker 0.08 mmol DPH was dissolved in 3 mL of EtOH and the solutions were mixed while stirring. The solution was then covered with parafilm, and placed in fume hood for slow evaporation at room temperature, where clear X-ray quality crystals of **3** were obtained after several days.

X-ray crystallography

Data collection and structure refinement details are summarized in Table 1. X-ray data were collected on a SMART X2S diffractometer using Mo-Kα radiation source. The crystal data was collected at -73 °C. A colorless needle crystal with dimensions of 0.20 x 0.20 x 0.60 nm was used for the X-ray analysis. The crystals were separated and lubricated in paratone-N oil which is used as an adhesive to mount the crystal on the Bruker spine pin. The structure was solved and refined using the SHELXTL software package. The final anisotropic full-matrix least-squares refinement on F2 with variables converged at R1, for the observed data and wR2 for all data. The goodness-of-fit, largest peak in the final difference electron density synthesis and the largest hole with an RMS deviation was considered. On the basis of the final model, the density and F(000) is calculated.

RESULT AND DISCUSSION

Structural studies

In this work we found that DPH can easily be protonated and crystalizes with several counter anions. In **1** the protonated compound crystallizes with a Cl^- counter anion along with three H_2O molecules in the lattice [17]. The compound crystallizes in monoclinic system and the space

group is $P2_1/n$. A hydrogen bond interaction is evident between a water molecule and the N atoms of the ligand with an O-N distance of 2.72 and 3.19 Å. The average C-N distances in the ring is 1.351 Å, while the average C-C distance in the aromatic ring system is 1.399 Å. The two CH_3 substituents at the 2- and 9- positions have C-C bond length of 1.490 Å. The structure exhibits intermolecular π–π stacking along the b-axis with neighboring π rings showing contacts as close as 3.6 Å.

Table 1. Crystallographic data of the DPH based compounds **1, 2**, and **3**.

Empirical formula	$C_{14}H_{20}ClN_2O_2$(**1**)	$C_{15}H_{12}F_3N_2O_3S$ (**2**)	$C_{16}H_{33}AuN_2O$ (**3**)
Formula weight	283.77	357.33	466.41
Temperature (K)	200(2)	200	199(2)
Crystal system	Monoclinic	Orthorhombic	Monoclinic
Space group	$P2_1/n$	$Pna2_1$	$P2_1/c$
Unit cell dimensions a (Å) b (Å) c (Å) β (°)	 12.6225(19) 7.2435(12) 16.087(2) 90.412(5)	 7.3536 (10), 18.454 (3) 11.6030 (18) 90	 a = 13.330(3) 15.667(3) 13.530(3) 109.98(6)
V ($Å^3$)	1470.8(4)	1574.6 (4)	2655.5(9)
Z	4	4	4
Density(calc) g/cm^3	1.281	1.507	1.167
Absorption coefficient mm^{-1}	0.260	0.255	5.540
Reflections collected	20041	11085	45661
Independent reflections R(int)	1902 (0.0979)	2152(0.06)	4726 (0.1825)
Data/restraints/parameters	1902 / 6 / 203	2152/1/220	4726 /0/ 347
Goodness-of-fit on F^2	1.213	1.03	1.206
Final R indices [I > 2sigma(I)]	R1 = 0.0438, wR2 = 0.1235	0.0372 0.106	0.0491 0.0842

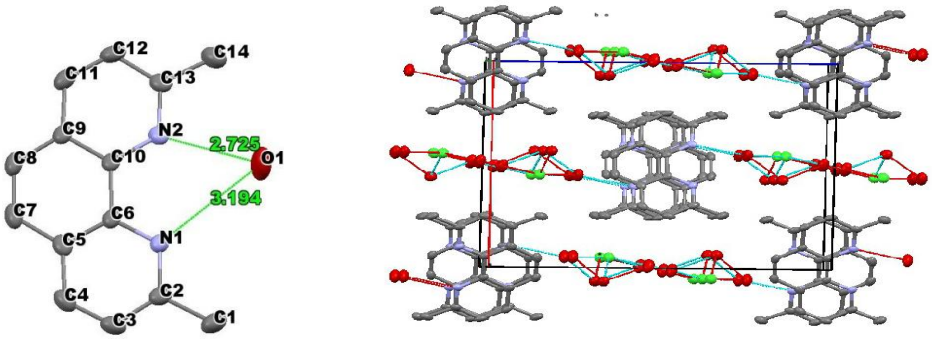

a) **b)**

Figure 1. X-ray crystal structure of **1** showing H-bonding interaction involving; a) a Cl^- anion, a H_2O molecule and the protonated N atom of the DPH molecule. The packing diagram in b) indicates the H-bonding network connecting the layers formed by pi-pi stacking.

The DPH molecules align themselves in antiparallel fashion with the two methyl substituents within the neighboring molecules pointing in the opposite direction. This π–π layer along the b-axis, is accompanied with a network of H-bonding interaction involving the Cl^- anion, water molecules and one of the protonated N atoms of the ligand. As shown in Figure 1, the H-bond interaction directed along the c-axis connects the layered π-stacking observed along the b-axis.

A strong H-bonding interaction between the protonated N and the oxygen atom of H_2O has been observed with an N-H---O distance of 2.725 Å as opposed to a weaker (3.194 Å) interaction with the other unprotonated N atom. Moreover, the average N-C distance for the protonated N atom increases by 0.016 Å when compared with the unprotonated N atom (1.359 vs 1.343 Å, respectively). In addition, the C-N-C angle at the protonated N site is larger than the corresponding angle at the unprotonated site (122.0^0 versus 117.7^0, respectively). Overall the structural data appears to indicate that both the distances and the angle around the protonated N site increases when compared with the unprotonated site.

The details of the H-bond interaction indicates that each Cl^- anion interacts with three water molecules in a Cl-H---O-H--Cl type arrangement at 3.198-3.220 Å distances and involve the protonated N atoms of the cation. In the front view of the packing diagram, the DPH molecules align themselves to create zig-zag channels. The H-bonding is directed perpendicular to the stacking layer, hence interconnects the layers providing additional stability to the solid state morphology.

The crystal structure of compound **2** is shown in Figure 2 and consists of the protonated ligand with a trifluoromethane sulfonate (triflate) counter anion. The compound has a molecular formula of $C_{15}H_{12}N_2SO_3F_3$ and crystallizes in an orthorhombic ($Pna2_1$) space group. Figure 2 shows a strong hydrogen bond interaction between the O atom of the triflate anion and one of the N atoms of the DPH ligand at a distance of 2.921 Å as opposed to a weaker (3.32 Å) interaction with the other unprotonated N atom. Hence, the N atom with a stronger H-bonding interaction is deduced as the protonated one. Moreover, the average N-C distance for the protonated N atom increases by 0.021 Å when compared with the unprotonated N atom (1.361 vs 1.339 Å, respectively). In addition, the C-N-C angle at the protonated N site is larger than the corresponding angle at the unprotonated site (123.2^0 versus 118.1^0, respectively). Overall the structural data indicates that both the distances and angle increase upon protonation in these systems.

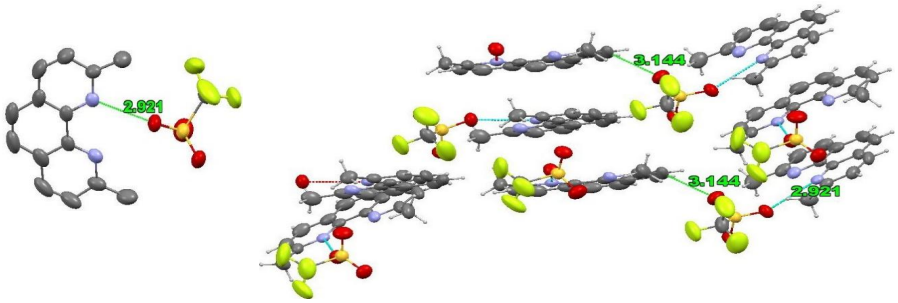

Figure 2. X-ray crystal structure of **2** showing H-bonding interaction involving the triflate anion, and the protonated N atom of the DPH molecule (left). The packing diagram on the right indicates the presence of H-bond directed intermolecular interaction involving intra-layer molecules. The H-bonding interaction does not involve inter-layer interaction formed by π-π stacking.

The average C-C bond distance within the ring system is 1.396 Å, while the C-CH_3 single bonds for the two methyl substituents are longer as expected at 1.465 and 1.483 Å. The crystal displays a face centered π-stacking of the ring system at distances as close as 3.14 Å along the a-axis. However, the stacking feature is different when compared with that of compound **1** indicating the influence of anions in directing the morphology of the solid state feature. The DPH molecules are arranged in such a way that alternate molecules aligned parallel to each other while neighboring groups are twisted by 40° when compared with the alternate molecular alignment. There is no extended H-bonding interaction involving H_2O molecules that connects the π–π stacked layers as was the case in compound **1**.

When the counter anion is changed to $Au(CN)_2^-$, the solid structural feature changes further as shown in Figure 3, where an unprotonated neutral molecule co-crystallizes along with the ionic system. Hence the structure of compound **3** consists of two DPH molecules, one counter anion and one H_2O molecule. The π–π interaction is also characterized by a feature where the terminal ring of one DPH molecule aligns with the central ring of the neighboring molecule. The interaction and the layer arrangement extend along the c-axis. Such alignment produces a π–π interaction close to 3.294 Å. The H_2O molecule in the structure is involved in H-bonding interaction with one of the N-atoms of the unprotonated DPH ring at 3.001 Å. In contrast, the protonated N atom is involved in H-bonding interaction with the N of the $Au(CN)_2^-$ anion at a N-H----NC distance of 2.985 Å. Moreover, similar to the trend observed in compounds **1**, and **2** the average N-C distance for the protonated N atom (Table 2) increases by 0.021 Å when compared with the unprotonated N atom (1.351 vs 1.335 Å, respectively). In addition, the C-N-C angle at the protonated N site is larger than the corresponding angle at the unprotonated site (121.9^0 versus 117.3^0, respectively). Hence a clear trend emerges where an increase in both bond distances and angle upon protonation is observed at the N site. The manner of π-stacking in compound **3** is different when compared to the other two compounds. As shown in Figure 3, the packing diagram indicates that the two methyl groups point in the same direction in an alternating parallel and anti-parallel pairs along the c-axis.

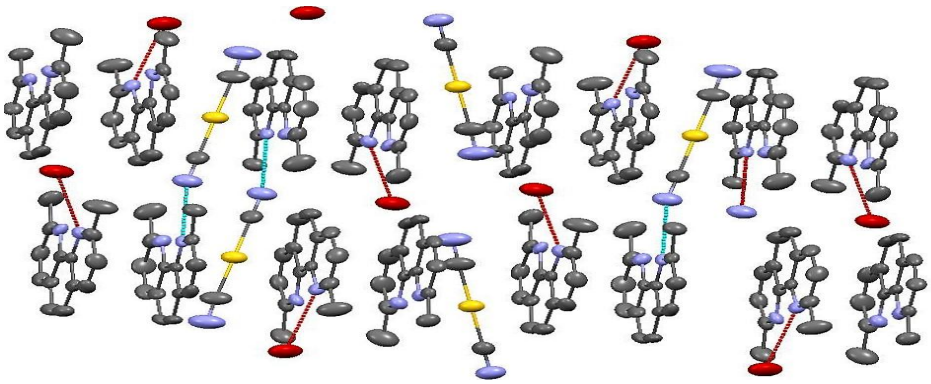

Figure 3. X-ray crystal structure of **3** showing alternating pairs of parallel and anti-parallel π-π stacking along the c-axis. The packing diagram also indicates the lack of an H-bonding involvement in interlayer interaction. The layers are formed through π-π stacking, which is the only major interaction to stabilize the solid state. The anion $Au(CN)_2^-$ displays H-bonding interaction with the ring containing the protonated N atom, although the structure lacks the well-known aurophilic [18], Au-Au interaction usually seen in gold(I) complexes.

Table 2. a) Selected bond lengths for **1**, **2**, and **3**, where the bond lengths around the N atoms are displayed. Comparison on the bond distances and the molecular interactions in the packing diagram indicates that the average N-C bond distance increases for the nitrogen atom which is involved in the H-bonding scheme. Hence, the underlined N atoms shown in the average column are deduced as the protonation sites for each compound. In Table b) the bond angles at the N sites are given. The C-N-C angle for all three compounds is larger at the protonation site as compared to the unprotonated N site. The atom numbering scheme was followed from the structural numbering scheme.

A)

Compound	Bond	Length (Å)	Average (Å)
1	N1-C6	1.358 (9)	
	N1-C2	1.329 (3)	1.343
	N2-C13	1.343 (9)	
	N2-C5	1.375 (3)	1.359
2	N1-C14	1.329 (9)	
	N1-C8	1.349 (3)	1.339
	N2-C7	1.375 (9)	
	N2-C2	1.346 (3)	1.360
3	N3-C24	1.366 (9)	
	N3-C16	1.336 (3)	1.351
	N4-C26	1.331 (9)	
	N4-C23	1.340 (3)	1.335

B)

Compound	Angles (^{0})
1, C13-N2-C10	122.0
C6-N1-C2	117.7
2, C2-N2-C7	123.2
C8-N1-C14	118.1
3, C16-N3-C24	121.9
C23-N4-C26	117.3

The observations indicated in the structural studies imply that certain factors might be essential in contributing to the stacking features in phenanthroline based systems [19-21]. Previous study on the related system, terpyridine, for example, indicated a similar observation that were rationalized in terms of position of the protonation at either the terminal N atoms or the central pyridine ring site. In [terpyH]-CF_3SO_3 [22, 23] for example, the terminal pyridine group was protonated, leading to π-stacking, while in [terpyH]PF_6 [22], protonation of the central pyridine group was found to lead to a random π–stacking feature.

The level of counter anion involvement in H-bonding interaction appears to influence the π-π stacking in this system. In this regard, the network of H-bonding interaction found in **2** is important in bringing stability in the solid state morphology [13-17]. In **3** where the H-bonding interaction of the $Au(CN)_2^-$ anion lacks to induce interlayer or intra-layer interaction, co-crystallization of the neutral molecule induces the needed π-π stacking that influences the crystal morphology. Similar behavior has been observed in previous structural work involving metal based anionic adducts including tetrachloridoferrate(III), Pt, and Ru containing anions [23-25].

Infrared studies

The IR spectra were collected on powder disk prepared by grinding X-ray quality single crystals and dried KBr. The vibrational spectra of compounds **1**, **2**, and **3** are shown in Figures 4a, b, and c, respectively. Common feature in **1** and **2** is the observance of the broad band at ~3460 cm^{-1} with a shoulder at the high energy side at ~3550 cm^{-1}. Splitting of this broad band is evident in **3**, where two well defined bands (Figure 4c) are observed at 3550 and 3450 cm^{-1}. The bands are assignable to a combination of ν_{NH} and ν_{OH} stretching, respectively, present due to protonation of the N atoms in these compounds as well as the presence of H_2O molecules involved in H-bonding interactions. The higher energy band at ~3550 cm^{-1} is absent in complexes where both N-atoms are directly coordinated to a metal center, supporting the assignment provided for the ν_{NH} stretching. As an example, in the IR spectrum of the $Cu(DPH)_2$(triflate).H_2O complex studied in our group, only a broad band at 3445 cm^{-1} is observed corresponding to the ν_{OH}

symmetrical stretch. The ν_{NH} symmetric stretch for the protonated N-site is observed at a higher wavenumbers when compared with the spectra for secondary and primary amines [26-27].

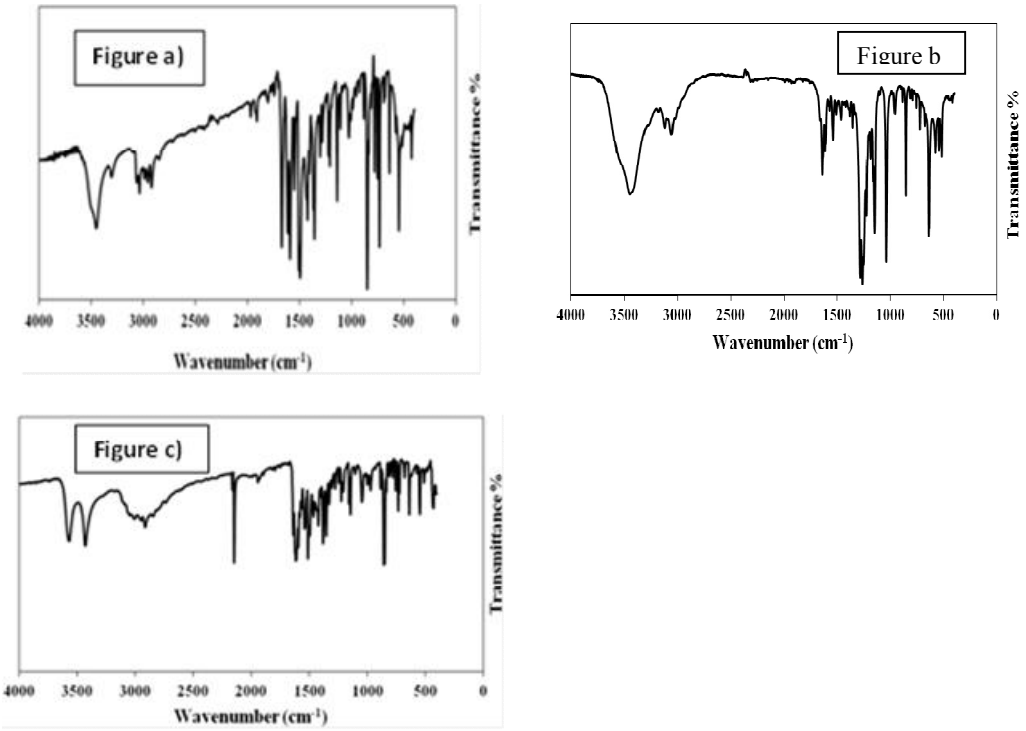

Figure 4. Infrared spectra of: a) compound **1**; b) compound **2**; and c) compound **3**.

A well-defined band is also observed at the lower energy side at ~3250 cm^{-1} in **1**, which appears as a very weak shoulder in **2**. Overlapping of the sp^2 hybridized ν_{CH} at 3035cm^{-1} and the sp^3 hybridized ν_{CH} at ~2980 cm^{-1} in all three compounds is due to the two types of protons in the DPH ligand. Moreover, compound **3** contains the characteristic ν_{CN} symmetric stretching at 2146 cm^{-1}. This value is typical of an uncoordinated $Au(CN)_2^-$ ion as is the case in simple salts like $KAu(CN)_2$ [28-29].

Luminescence studies

The luminescence property of the DPH molecule has been investigated previously and was found to emit weakly upon UV excitation [30, 31]. The emission maxima were also found to depend on the pH of the solution. The neutral molecule was found to undergo a $\pi \rightarrow \pi^*$ transition and emits at ~360 nm. The protonated molecule in mildly acidic condition was found to emit at redshifted position of ~410 nm. In this study where emission property in the solid state wereinvestigated, compound **1** emits at ~395 nm, with a slight blue shift when compared with that of the acidic solution. The excitation spectrum also maximizes at 329 nm. Never the less its value is consistent with the protonation of the compound. Similar profile was also observed in compound **2**. In contrast, compound **3** was thought to display the influence of a transition metal

anion on the spectroscopic property of the DPH core. The solid emission spectrum of **3** is compared with that of the unprotonated ligand in Figure 5. The emission profile is very similar to the emission of the protonated ligand, and hence suggests that the frontier orbitals in this complex are largely ligand based with minimal effect from the metal contribution. Consistent with its structural feature, no emission assignable to Au-Au interaction [32-35] has been observed in compound **3**.

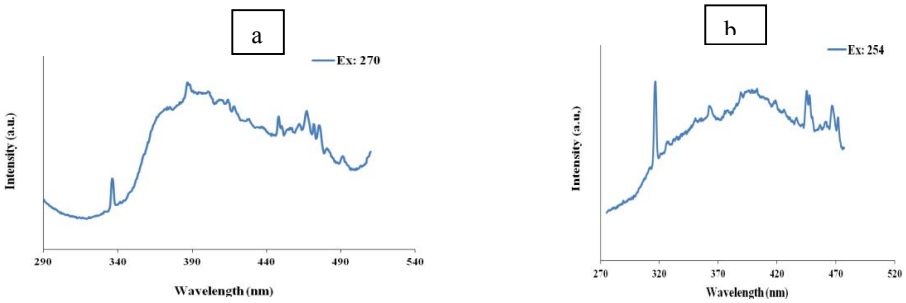

Figure 5. Emission spectrum of: a) neutral unprotonated ligand; b) compound **3** collected at room temperature upon excitation with 245 nm. The sharp bands are instrumental artifacts.

CONCLUSION

Three crystal structures of the pronated ligand, 2,9-dimethyl-1,10-phenanthrolin1ium (DPH) cation with selected counter anions (chloride, triflate, and gold dicyanide) are characterized crystallographically. The role of a hydrogen bond interaction in stabilizing the solid state π-π interaction was investigated. In all three compounds the π-π interaction was evident. In compounds **1** and **2** the solid state morphology was stabilized by additional H-bonding interaction. In particular, compound **1** displays extensive network of H-bonding interaction where π–π stacked layers are interlinked through the H-bonding network. In compound **2**, the H-bonding interaction is less pronounced and involves mainly the non-coordinating triflate anion and the protonated N atom of the DPH molecule. In contrast compound **3** shows minimal anion interaction and additional stability is attained through co-crystallization of a neutral phenanthroline group. Moreover, the emission behavior is unaffected by the counter anion change indicating that the frontier orbitals involved in the electronic transitions in all three compounds are largely DPH based orbitals.

ACKNOWLEDGEMENT

Support for this research from National Science Foundation (CHE-0959406) and as well as support from the donors of the Petroleum Research Fund are kindly acknowledged.

REFERENCES

1. Summers, L.A. *Adv. Heterocycl. Chem*. **1978**, 22, 1.
2. Sammes, P.G.; Yahioglu, G. *Chem. Soc. Rev*. **1994**, 23, 327.
3. Luman, C.R.; Castellano, F.N.; McCleverty, J.A.; Meyer, T.J.; Lever, A.B.P. (Eds.) *Comprehensive Coordination Chemistry*, Vol. 1, Elsevier: Oxford, UK; **2004**; p 25.
4. Bencini, A.; Lippolis, V. *Coord. Chem. Rev*. **2010**, 254, 2096.
5. Chelucci, G.; Addis, D.; Baldino, S. *Tetrahedron Lett*. **2007**, 48, 3359.

6. Xu, H.; Wei, Y.; Zhao, B.; Huang, W. *J. Rare Earths* **2010**, 28, 666.
7. Anderegg, G. *Helv. Chim. Acta* **1963**, 46, 2397.
8. Anderegg, G. *Helv. Chim. Acta* **1963**, 46, 2813.
9. Paoletti, P. *Pure Appl. Chem.* **1984**, 56, 491.
10. Beech, G.; Ashcroft, S.F.; Mortimer, C.T. *J. Chem. Soc. A-Inorg. Phys. Theor.* **1967**, 6, 929.
11. Choppin, G.R.; Peterman, D.R. *Coord. Chem. Rev*. **1998**, 174, 283.
12. Elbanowski, M.; Mąkowska, B. *J. Photochem. Photobio*. *A-Chem*. **1996**, 99, 85.
13. Taydakov, I.V., Zaitsev, B.E., Krasnoselskiy, S.S., Starikova, Z.A. *J. Rare Earths* **2011**, 29, 719.
14. Zhong, K.-L. *Acta Cryst.* **2013**, E69, o1782.
15. Arman, H.D.; Kaulgud, T.; Tiekink, E.R.T. *Acta Cryst*. **2013**, E69, o1445.
16. Derikvand, Z.; Olmstead, M.M. *Acta Cryst*. **2011**, E67, O87-U2099.
17. Yu, Y.-Q., Ding, C.-F., Zhang, M.-L., Li, X.-M.; Zhang, S.-S. *Acta Cryst.* **2006,** E62, o2187.
18. Schmidbaur, H.; Schier, A. *Chem. Soc. Rev*. **2008**, 37, 1931.
19. Gomleksiz, M.; Cihan Alkan, C.; Erdem, B. *Bull. Chem. Soc. Ethiop*. **2013**, 27, 213.
20. Samadi, N.; Salamati, M. *Bull. Chem. Soc. Ethiop*. **2014**, 28, 373.
21. Bencinia, A.; Lippolisb, V. *Coord. Chem. Rev.* **2010,** 254, 2096.
22. Yoshikawa, N.; Yamabe, S.; Kanehisa, N.; Takashima, H.; Tsukahara, K. *J. Phys. Org. Chem*. **2009**, 22, 410.
23. Noruzi, E.B.; Safari, N.; Amani, V.; Notash, B. *Acta Cryst.* **2012**, E68, m905.
24. Yousefi, M.; Ahmadi, R.; Amani, V.; Khavasi, H.R. *Acta Cryst*. **2007**, E63, m3114.
25. Moreno, M.A.; Haukka, M.; Kallinen, M.; Pakkanen, T.A. *Appl. Organomet. Chem.* **2006**, 20, 51.
26. Al-Sehemi, A.G.; Saied, R.; Al-Amri, A.A.; Irfan, A. *Bull. Chem. Soc. Ethiop.* **2014**, 28, 111-120
27. Al-Sehemi, A.G.; Irfan, A.; Asiri, A.M.; Ammar, Y.A. *Bull. Chem. Soc. Ethiop*. **2015**, 29, 137.
28. Stammreich, H.; Chadwick, B.M.; Frankiss, S.G. *J. Mol. Struct*. 1967-1968, I, 191.
29. Chadwick, B.M.; Frankiss, S.G. *J. Mol. Struct*. **1976**, 31, 1.
30. Henry, M.S.; Hoffman, M.Z. *J. Phys. Chem.* **1979**, 83, 5, 618.
31. Azumi, T.; McGlynn, S.P. *J. Chem. Phys*. **1962**, 37, 2413.
32. Assefa, Z.; Shankle, G.; Patterson, H.H.; Reynolds, R. *Inorg. Chem*. **1994**, 33, 2187.
33. Assefa, Z.; DeStefano, F.; Garepapaghi, M.A.; LaCasce, J.H., Jr.; Ouellete, S.; Corson, M.R.; Nagle, J.K.; Patterson, H.H. *Inorg. Chem*. **1991**, **30**, 2868.
34. Ladner, L.; Ngo, T.; Crawford, C.; Assefa, Z.; Sykora, R.E. *Inorg. Chem*. **2011,** 50, 2199
35. Smith, P.A.; Crawford, C.; Beedoe, N.; Assefa, Z.; Sykora, R.E., *Inorg. Chem*. **2012**, 51, 12230.